

Selective CO Oxidation on a Ru/Al₂O₃ Catalyst in the Surface Ignition Regime: 1. Fine Purification of Hydrogen-Containing Gases¹

A. Ya. Rozovskii, M. A. Kipnis, E. A. Volnina, P. V. Samokhin, and G. I. Lin

Topchiev Institute of Petrochemical Synthesis, Russian Academy of Sciences, 119991 Russia

e-mail: rozovsk@ips.ac.ru

Received January 31, 2006; in final form, June 21, 2007

Abstract—Selective CO oxidation in a mixture simulating the methanol steam reforming product with an air admixture was studied over Ru/Al₂O₃ catalysts in a quasi-adiabatic reactor. On-line monitoring of the gas temperature in the catalyst bed and of the residual CO concentration at different reaction conditions made it possible to observe the ignition and quenching of the catalyst surface, including transitional regimes. A sharp decrease in the residual CO concentration takes place when the reaction passes to the ignition regime. The evolution of the temperature distribution in the catalyst bed in the ignition regime and the specific features of the steady-state and transitional regimes are considered, including the effect of the sample history. In selective CO oxidation and in H₂ oxidation in the absence of CO, the catalyst is deactivated slowly because of ruthenium oxidation. In both reactions, the deactivated catalyst can be reactivated by short-term treatment with hydrogen. A 0.1% Ru/Al₂O₃ catalyst is suggested. In the surface ignition regime, this catalyst can reduce the residual CO concentration from 0.8 vol % to 10–15 ppm at O₂/CO = 1 even in the presence of H₂O and CO₂ (up to ~20 vol %) at a volumetric flow rate of ~100 l(g Cat)⁻¹ h⁻¹, which is one magnitude higher than the flow rates reported for this process in the literature.

DOI: 10.1134/S0023158408010114

In recent decades, there have been extensive studies on the catalytic removal of CO from hydrogen-containing gases (selective CO oxidation). This interest is due to the development of technologies using H₂ in electricity generation (fuel processors), separation processes using platinum metal membranes, etc. As a rule, fuel processors require that CO in the hydrogen-containing gas be reduced to 10–100 ppm. A promising solution to this problem is use of catalysts based on noble metals, in particular, Ru-containing catalysts [1–7].

A possible source of hydrogen is methanol [1, 2, 7, 8]. Methanol steam reforming yields a gas containing hydrogen, ~1% CO, ~20% water, and CO₂. This gas is purified from CO by oxidizing the latter into CO₂. In order to achieve a low residual CO level at high flow rates, CO is removed in two steps (or more) [8–10] with oxygen introduction between the stages or the O₂/CO ratio is raised. However, two-step purification complicates the overall process (since it requires CO and O₂ control between the stages, an extra air feed, and a larger volume of the CO converter). Raising the O₂/CO ratio leads to extra oxygen consumption for hydrogen oxidation and, hence, a lower capacity of the fuel processor.

Since oxygen is also spent on hydrogen oxidation, its proportion in the gas mixture should be above the stoichiometric proportion. The normal reactant ratio seems to be O₂/CO = 1. In fact, the desired reduction of the CO content in the case of ruthenium catalysts is usually achieved at O₂/CO > 1 [2–6, 8, 10–12], at a low or zero water content [1, 6, 13], and at moderate GHSV values (no higher than 15000 h⁻¹) [2–4, 7, 12]. At a low CO content of hydrogen (0.6 vol %), in the absence of water and CO₂, and a low GHSV of 7500 h⁻¹, the desired purification efficiency can be achieved at O₂/CO = 1 [6]. However, if the CO concentration in the initial mixture is raised from 0.6 to 1%, it will be necessary to increase the O₂ content from 0.6 to 1.5 vol % in order to reduce the residual CO content to the desired level of 10 ppm [6].

In vehicular applications of fuel cells, the catalyst has to operate at rather high gas flow rates. To ensure an electric power of 10 kW, the methanol steam reforming products must be passed through the fuel processor at a rate of 200 l/min [8]. If the desired power is one magnitude higher, which is the case for modern automobiles, the required flow rate will be ~100 m³/h. At GHSV values usual for catalytic processes (~10000 h⁻¹ and below), CO removal from this amount of the gas

¹ The article includes materials from the authors' report at the II Russian Conference on Current Problems in Petroleum Chemistry, Ufa, October 11–13, 2005.

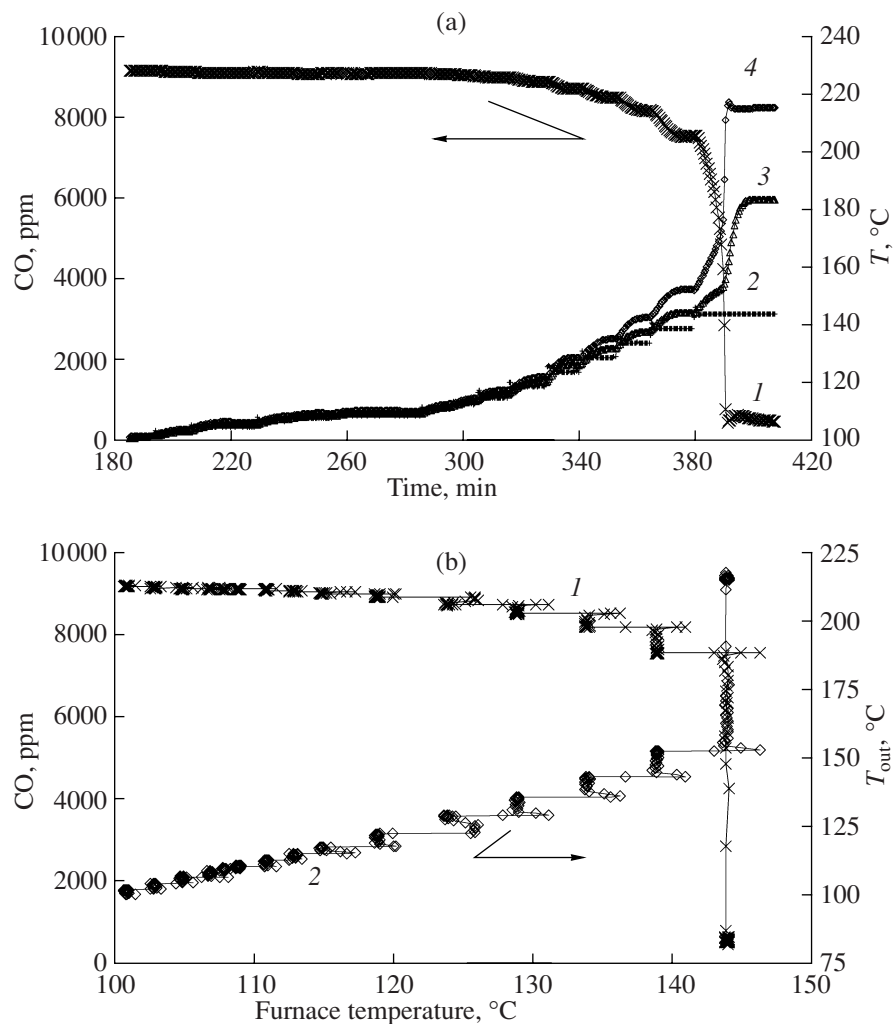


Fig. 1. Selective CO oxidation on the 1% Ru/Al₂O₃ catalyst. Fragment of a record of the process made while heating the surface in steps: (a) dynamics of (1) the residual CO concentration, (2) the furnace temperature, (3) the gas temperature at the catalyst bed entrance, and (4) the gas temperature at the bed exit; (b) (1) residual CO concentration and (2) gas temperature at the bed exit versus the furnace temperature. Feed composition (vol %): CO, 0.75; O₂, 0.75; H₂, 57; CO₂, 18; H₂O, 20; N₂, balance. The gas flow rate is 87 l (g Cat)⁻¹ h⁻¹.

will require a catalyst volume of ~10 l. Since almost complete CO removal is required, the real catalyst volume will be much larger.

Thus, a challenging problem is to design a highly active and selective catalyst capable of removing CO at high GSHV values and in the presence of H₂O and CO₂.

In earlier studies [14, 15], we demonstrated by the example of a modified platinum catalyst that the purification efficiency can be significantly raised by conducting selective CO oxidation in the catalyst surface ignition regime (the specific features of chemical reactions in this regime are considered in earlier monographs [16, 17]).

Here, we report our study of selective CO oxidation on ruthenium catalysts. By combining an active catalyst with a favorable macrokinetic regime, we have

achieved a high-purity product at O₂/CO = 1 and flow rates of about 100 l (g Cat)⁻¹ h⁻¹.

EXPERIMENTAL

Catalyst Synthesis

The catalyst support was commercial γ-Al₂O₃ extrudate (Ryazan Refinery, A-64k brand, specific surface area of 200 m²/g, size fraction of 0.200–0.315 mm after crushing). Before loading the active component, the support was calcined in air at 500°C for 2 h. The starting ruthenium compound was Ru(OH)Cl₃ (see the caption to Fig. 5). Catalysts were prepared by impregnating alumina with a ruthenium salt solution followed by drying at 120°C for 6 h. After being charged into the reactor (without an inert

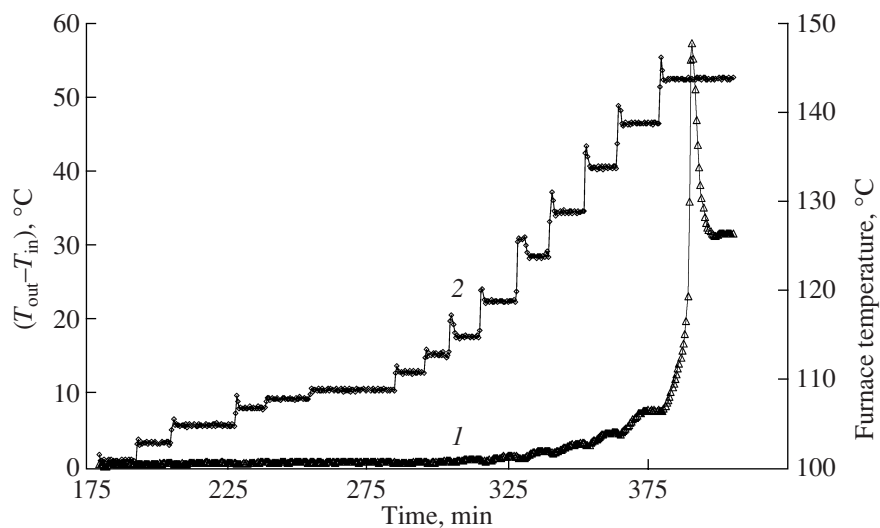


Fig. 2. Catalyst bed heating dynamics in selective CO oxidation on the 1% Ru/Al₂O₃ catalyst: (1) difference between the gas temperatures at the bed exit and entrance and (2) furnace temperature. The process conditions are the same as in Fig. 1.

component), the catalyst was reduced in flowing H₂ (3.5 l/h) for 2.5 h at 350 or 400°C.

Gas Mixtures

The gas mixtures to be used in experiments were prepared by the partial pressure method from H₂ (RF Specifications 6-20-00209585-26-07), CO₂ (USSR State Standard GOST 8050-85), N₂ (USSR Specifications TU 6-21-39-79, grade B), O₂ (USSR State Standard GOST 5583-78, grade 1), and CO obtained by formic acid decomposition. Vapor–gas mixtures used in selective CO oxidation simulated the methanol steam reforming product (H₂, ~55–60 vol %; CO, ~0.8 vol %; CO₂, ~20 vol %; H₂O, ~20 vol %). Oxygen was usually

added to this mixture as the oxidizer so that the initial CO/O₂ ratio was 1 : 1. Furthermore, a mixture of H₂, O₂, and N₂ was used to study the specific features of H₂ oxidation.

IR gas analyzers were calibrated and tested against standard gas mixtures from the Balashikha Oxygen Works, including mixtures containing less than 100 ppm CO.

Catalytic Tests

Catalytic activity was studied using a modified variant of the quartz flow reactor described in [15].

As compared to its previous version [15], the reactor had a sealed-in porous quartz partition for supporting the catalyst bed and a bypass line with two three-way valves for bypassing the gas when necessary.

Experiments were performed at atmospheric pressure. The initial gas mixture was fed into the reactor through a unit allowing the gas flow rate to be measured and regulated. The flow rate was varied in the range of 60–300 ml/min. The flow rate of the dry gas was measured with an IRG-1000 flowmeter with a scale interval of 1 ml/min.

The gas mixture resulting from the reaction was dried at 0°C and was divided into two streams with metering valves. One stream was analyzed chromatographically for CO, CH₄, and O₂ (LKhM 80 chromatograph, thermal-conductivity detector, zeolite 13X column, O₂ detection limit of ~20 ppm, CH₄ detection limit of ~40 ppm, CO detection limit of ~100 ppm). The second stream was directed to a BINOS 100 dual-channel IR gas analyzer to quantify CO (measurement range of 0–9999 ppm) and CO₂ (measurement range of 0–25%, relative error no greater than 5%). The error of CO determination in the gas was mainly determined by

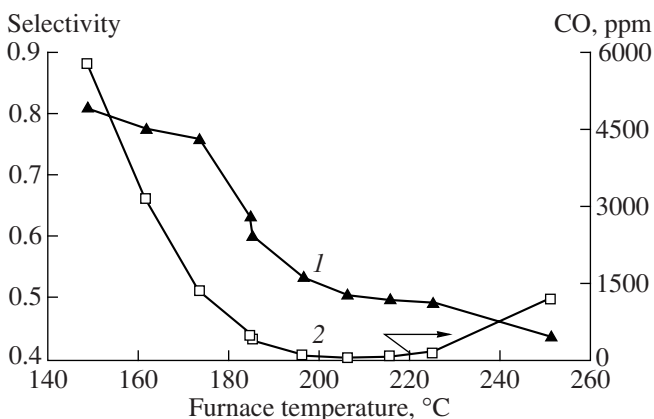


Fig. 3. Temperature dependence of the reaction selectivity for CO oxidation in an isothermal reactor on the 0.1% Ru/Al₂O₃ catalyst: (1) oxygen consumption selectivity and (2) residual CO concentration. The feed composition is the same as in Fig. 1. The gas flow rate is 90 l(g Cat)⁻¹ h⁻¹.

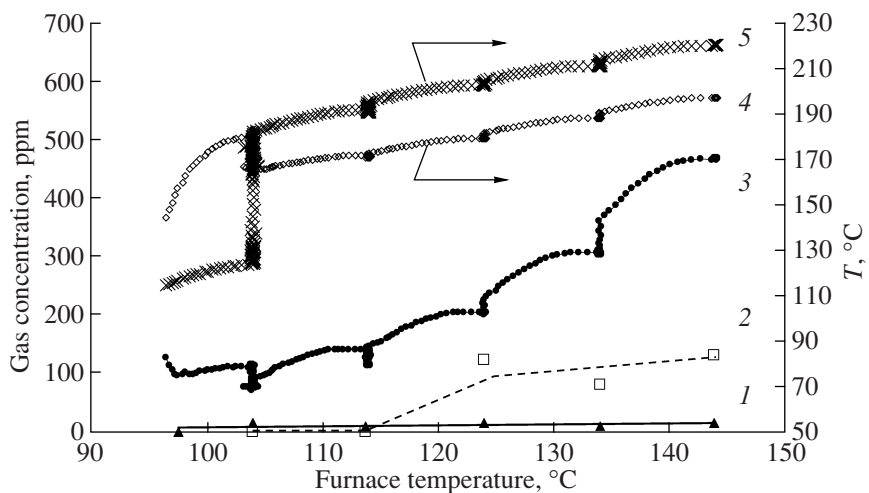


Fig. 4. Selective CO oxidation on the 1% Ru/Al₂O₃ catalyst in the catalyst surface ignition regime during the stepwise cooling of the furnace: (1–3) outlet O₂, CH₄, and CO concentrations, respectively; (4, 5) gas temperatures at the bed exit and entrance, respectively. The feed composition is the same as in Fig. 1. The gas flow rate is 91 l (g Cat)⁻¹ h⁻¹.

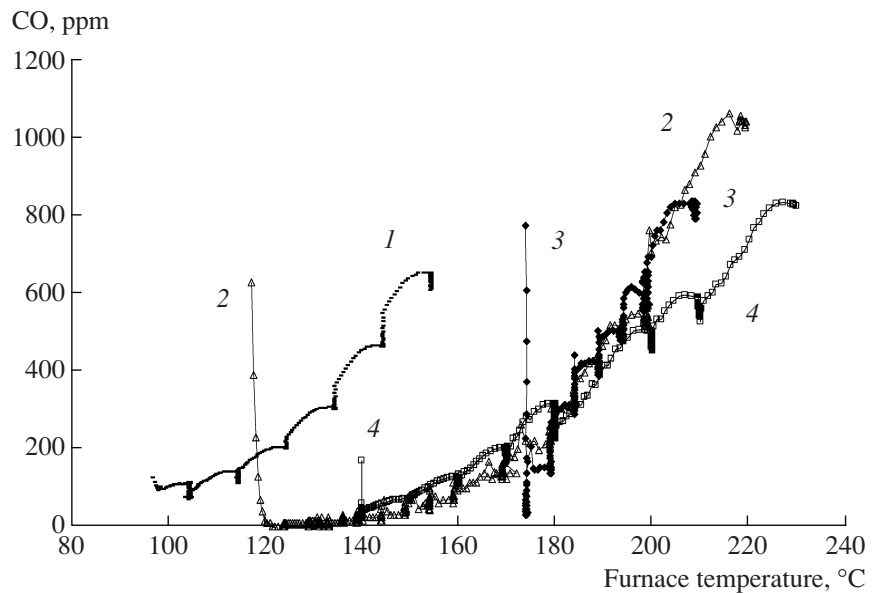


Fig. 5. Residual CO concentration in selective CO oxidation on (2–4) 0.1% Ru/Al₂O₃ low-percentage catalysts as compared to (1) 1% Ru/Al₂O₃ in the catalyst surface ignition regime during the stepwise cooling of the surface. The feed composition is the same as in Fig. 1. The gas flow rate is 91 l (g Cat)⁻¹ h⁻¹.

the error in the composition of the calibration mixtures and by the baseline drift. At low CO concentrations (~20 ppm), it was ≤ 2 ppm.

Current values of the CO concentration (in 1 ppm increments) and CO₂ concentration (in 0.1% increments) were displayed on the IR analyzer. The analog signal from the CO channel was directed to a five-channel measuring controller (designed by A.P. Manyakin). This device was also used to monitor the furnace and catalyst temperatures (± 0.1 K) and control the furnace

temperature. The gas temperature in the catalyst bed was measured with two thermocouples placed at the bed entrance and exit, each at a distance of 1–2 mm from the bed surface. The bed thickness was 1.2–1.4 cm, and the catalyst weight was ~0.2 g.

When there was no reaction, the steady-state readings from the thermocouples differ insignificantly (by a few tenths of a degree Celsius). At the furnace temperatures 110°C and 250°C, they differ from the reading from the control thermocouple by 2.5 and 7°C, respectively.

A special-purpose program (written by A.S. Korotkov) allowed on-line computer monitoring of the parameters being measured.

Prior to experiments, the reactor was tested for tightness by pressurization and was then heated in an H_2 flow (3.5–4.0 l/h) to the preset temperature. Next, water was fed into a preheated evaporator and hydrogen was replaced with the reaction mixture by switching the flows with a Swagelok five-way valve. After the experiment, the reactor was purged with hydrogen and the catalyst was left under a hydrogen pressure.

RESULTS AND DISCUSSION

Specific Features of the Reaction under Ignition Conditions: Transitional Regimes

The CO and H_2 oxidation reactions are very exothermic ($\Delta H = -283.0$ and -241.8 kJ/mol, respectively [12]). In a quasi-adiabatic reactor, these reactions readily pass to a catalyst surface ignition macrokinetic regime [16, 17]. This transition usually takes place abruptly. It can be observed as a dramatic rise of the gas temperature in the catalyst bed and as a decrease in the residual CO content of the gas mixture.

Figure 1a shows fragments of the residual CO, furnace temperature, and the entrance and exit gas temperatures for the 1% Ru/ Al_2O_3 catalyst bed (stepwise heating in 5 K increments, 10- to 20-min-long arrests at each temperature point). Figure 1b plots the residual CO content and the gas temperature at the bed exit versus the furnace temperature.

As is clear from these plots, raising the furnace temperature up to 139°C causes a temperature rise in the catalyst bed and a decrease in the residual CO content. Raising the furnace temperature from 139 to 144°C causes the ignition of the catalyst surface. This is manifested as a dramatic increase of the catalyst bed temperature and as a sharp decrease in the residual concentrations of CO (down to ~490 ppm) and O_2 (according to chromatographic data, the oxygen conversion is as high as 99.6%). The gas temperature at the exit of the catalyst bed under the ignition conditions was 215°C.

Let us consider the catalyst heating dynamics in this experiment in greater detail (Fig. 2). As the furnace temperature is raised in steps from 115 to 139°C, the difference between the bed exit and entrance temperatures increases monotonically from 1 to 7.8 K, stabilizing at each step. By contrast, raising the temperature by another 5 K, from 139 to 144°C, causes the catalyst surface to ignite. The difference between the bed exit and entrance temperatures is as large as 57.5 K at the ignition point and stabilizes at 31.8 K in the steady-state region.

The presence of a sharp peak in the heating dynamics curve (Fig. 2) deserves special consideration. For very exothermic reactions with a positive reaction order, the heat-induced ignition of the catalyst surface should take place at low conversions, when the reaction

rate and, accordingly, the heat evolution rate are the highest. In this case, it is obvious that, under preignition conditions, the maximum temperature (hot spot) will occur at the downstream end of the catalyst bed. It is also obvious that the critical ignition conditions will primarily be established around the hot spot to enhance the CO conversion and heat evolution. Owing to the longitudinal transfer of the extra heat and the corresponding perturbation, the ignition regime gradually propagates in the bed as long as the perturbation intensity is sufficient for satisfying the critical ignition conditions for a given cross section. Note that the rate of this process depends not only on the rate of heat transfer through the reactor walls, but also on the mass flow rate of the gas mixture in the reactor, because part of the extra heat transferred to a reactor cross section is spent on the heating of the gas coming to this cross section.

Thus, the ignition of the catalyst surface begins at the bed exit and the ignition zone gradually expands toward the upstream end of the bed. As the ignition zone propagates to the upstream end, the CO and O_2 conversions increase. Accordingly, the CO and O_2 concentrations at the bed exit decrease to slow down the oxidation reaction and to reduce the heat evolution due to these reactions at the bed exit. The hot spot thus shifts toward the bed entrance.

In a steady state, nearly all of the oxygen around the hot spot is reacted. Therefore, moving further along the reactor axis, the gas mixture only cools down because of heat transfer through the reactor walls.

These features determine the dynamics of the longitudinal temperature distribution in the catalyst bed: in an unsteady state, a dramatic surge of the temperature difference ($T_{out} - T_{in}$) is observed immediately after ignition. After that, the temperature difference gradually decreases to the value characteristic of the steady-state regime. The transitional period in our experiment was ~7 min long.

The reverse behavior will be observed in surface quenching. For example, if quenching is initiated by furnace cooling or by catalyst deactivation, the hot spot will move toward the bed exit, followed by the ignition zone boundary moving in the same direction.

Effect of Temperature on the Oxidation Selectivity

The effect of temperature on the selectivity of oxygen consumption in CO oxidation in a steady-state regime (0.1% Ru/ Al_2O_3 , sample 2; see caption to Fig. 5) was studied in an isothermal stainless steel flow reactor using a KL-3D setup (designed by the Design Office of the Zelinskii Institute of Organic Chemistry, Russian Academy of Sciences). The catalyst batch was diluted with a tenfold volume of quartz (0.25–0.315 mm size fraction) and was placed into the annular space between the reactor walls and the thermocouple well. The residual CO and O_2 concentrations were determined chromatographically.

The results obtained in this experiment are presented in Fig. 3. As the temperature is raised, the oxidation selectivity decreases from a near-stoichiometric value to 0.5 (Fig. 3, curve 1), forming a plateau, and then to lower values. The plateau at ~190–230°C corresponds to the so-called “window” in which the lowest residual CO concentration is observed. As the temperature is further raised, the residual CO concentration increases at a rather high, progressively increasing rate and, accordingly, the oxygen consumption selectivity decreases.

*Initiation of the Reaction
above the Critical Ignition Temperature*

The simplest way of establishing the ignition regime is by admitting the reaction mixture into a reactor preheated to a temperature well above the critical ignition temperature of the catalyst surface (T_{cr}). In this case, the ignition regime will be established immediately after the admission of the feed. The larger the difference $T - T_{cr}$, the shorter the time required for the establishment of a steady-state regime.

In the ignition regime, the furnace temperature may be reduced well below the critical ignition temperature (down to the critical surface quenching temperature) without breaking down this regime. This provides a means of enhancing the oxygen consumption selectivity.

Figure 4 illustrates the dynamics of the component concentrations and gas temperature at the entrance and exit of the 1% Ru/Al₂O₃ bed during a stepwise decrease of the furnace temperature with 10- to 20-min-long temperature arrests. In this experiment, the reactor was preheated to 144°C in flowing H₂, and the hydrogen flow was then replaced with a feed flow. This caused the ignition of the catalyst surface. The residual CO concentration was ~470 ppm, and the O₂ conversion was ~99.9%. The highest gas temperature in the steady-state surface ignition regime was observed near the bed entrance and was 220°C (versus 197°C at the bed exit).

Next, we began to cool the furnace, making temperature arrests at 134, 124, 114, and 104°C.

As the furnace was cooled, the residual CO concentration decreased to ~100 ppm. Oxygen was consumed almost completely throughout the temperature range until the quenching of the surface, which begins $\geq 104^\circ\text{C}$. Thus, under conditions of the experiment considered, temperature reduction in the ignition regime is favorable for selective CO oxidation. This is in agreement with the data obtained for an isothermal reactor using a low-percentage catalyst (Fig. 3).

When the gas temperature at the exit of the catalyst bed is $> 200^\circ\text{C}$, the desired oxidation reaction is accompanied by methane formation (Fig. 4). On the ruthenium catalysts, methane results from CO hydrogenation. As the temperature is raised, the contribution from this reaction to the overall CO conversion increases. The hydrogenation of CO, not CO₂, was proved by

hydrogenating a CO + CO₂ mixture. It was found that the reaction between hydrogen and CO₂ begins only after the disappearance of CO. When the gas temperature in the catalyst bed is $< 200^\circ\text{C}$, no methane is detected among the reaction products.

The longitudinal temperature profile in the catalyst bed for the experiment whose results are presented in Fig. 4 is different from the profile shown in Fig. 1: the hot spot is shifted toward the bed entrance, so that the gas temperature near the entrance cross section exceeds the gas temperature at the bed exit until the catalyst surface is quenched.

Holding the catalyst bed at 104°C for 70 min shifted the hot spot toward the bed exit. Further cooling of the furnace caused a marked decrease in the gas temperature in the catalyst bed: the quenching of the catalyst surface set in.

*Effect of the Reaction “Start” Temperature
on the Macrokinetic Situation in the Catalyst Bed
Operated in the Ignition Regime*

As follows from the above, the axial temperature distribution in a flow reactor for selective CO oxidation depends on how the reaction was initiated, namely, by starting it directly above the critical catalyst ignition temperature (T_{cr}) or by gradually bringing it to this temperature “from below.”

We have already considered the establishment of the ignition regime in a flow reactor by gradual heating. This regime usually “nucleates” in the vicinity of a hot spot (which usually occurs near the bed exit because of the low conversion) and then propagates toward the bed entrance owing to longitudinal heat transfer, gradually occupying all or part of the catalyst bed.

When the system is brought to the ignition regime “from above” (that is, from a temperature far exceeding T_{cr} , as in the experiment illustrated in Fig. 4), this regime is rapidly established in the upstream part of the bed. Subsequently reducing the temperature will not quench the catalyst surface in the upstream layers until the critical quenching temperature (T_{quench}) is reached. Since the quenching temperature is well below T_{cr} (the difference is tens of degrees), there is some interval $T_{quench} < T < T_{cr}$ in which different regimes can simultaneously exist (or, as is probably more correct, coexist) under the same conditions. Indeed, the surface ignition regime established at a higher temperature will persist in the upstream part of the bed if the temperature is decreased within this interval. At the same time, if the system is brought to ignition from lower temperatures, it is possible that the ignition regime will not be established in the upstream part of the bed because of the insufficient longitudinal heat flux in the direction opposite to the gas flow direction.

As a consequence, under given external conditions, the system in which the ignition regime was established at a high temperature and in which this temperature was

then reduced may be nonidentical to the system in which the ignition regime was established by a gradual temperature rise. Here, we deal with one more memory effect in heterogeneous catalysis, which, however, arises from pure macrokinetic features of the system.

Effect of the Properties of the Catalyst on the CO Oxidation Selectivity

Along with 1% Ru/Al₂O₃, a series of low-percentage catalysts containing 0.1 wt % Ru was prepared and tested. Under the conditions of selective CO oxidation, we observed surface ignition for all catalyst samples. Figure 5 plots the residual CO content versus the furnace temperature in the catalyst surface ignition regime for three samples prepared by different methods.² For comparison, we present data for the 1% Ru catalyst. Equal weights of the four samples were tested. In all runs, the sample was heated in flowing hydrogen to a temperature exceeding the critical ignition temperature and the feed was then admitted.

As is clear from the plots shown in Fig. 5, the low-percentage catalysts are much less active than the 1% Ru catalyst. A given CO conversion is achieved on the former at temperatures ~50 K higher than on the latter. Oxygen is converted almost completely in the ignition regime. The reaction over the low-percentage catalysts yields no methane.

The effect of the oxidation temperature on the selectivity of the reaction in the ignition regime is the same as is described above: reducing the temperature causes a decrease in the residual CO concentration until the quenching of the surface. Therefore, the lower the surface quenching temperature for a given catalyst, the lower the residual CO level attainable by oxidation. The surface quenching temperature in the low-percentage catalyst series varies in a wide range (Fig. 5), and it is, therefore, possible to achieve much lower residual CO levels than are attainable with the 1% Ru catalyst.

Note that, in the catalyst surface ignition regime, the reaction is controlled by external diffusion. It might be expected that, in this case, the nature of the catalyst will have no effect on the reaction kinetics and even selectivity because the hydrogen concentrations at the catalyst surface and in the flow core are approximately equal. In fact, the catalyst composition effect is quite evident (Fig. 5). As follows from the above discussion, this effect is mediated by the effect of the catalyst composition on the surface quenching temperature. In turn, the latter effect makes it possible to carry out the oxidation process at a lower temperature within the ignition limits and thus enhance the selectivity of the reaction.

² Samples 1, 3, and 4 were synthesized by impregnating alumina with an aqueous solution of the ruthenium salt. For samples 1 and 3, the solution was maintained at pH 10. Sample 2 was synthesized by vacuum impregnation with a toluene solution of a metal complex prepared from the original ruthenium salt and trioctylamine [18].

Thus, we have got another means of controlling the selectivity of the process in the catalyst surface ignition regime.

Stability of the Ruthenium Catalysts

The enhanced selectivity effect in CO oxidation in the catalyst surface ignition regime is rather stable. Nevertheless, it is known from the literature that ruthenium catalysts undergo comparatively rapid deactivation in CO oxidation. In CO + O₂ + He mixtures (CO/O₂ = 0.5, 2, 4) reacting on a Ru/SiO₂ catalyst heated in steps to 140°C, the CO conversion at each temperature point decreased rather soon (within a few tens of minutes); furthermore, the CO conversion was lower during stepwise cooling than during stepwise heating [19]. According to in situ IR spectroscopic data, the intensities of the absorption bands due to CO linearly adsorbed on metallic ruthenium (2010 and 2030 cm⁻¹) and on oxidized ruthenium (2080, 2130, and 2135 cm⁻¹) increased monotonically at 100°C. Raising the temperature caused a weakening of all the absorption bands. A possible cause of catalyst deactivation is that ruthenium oxides reacting sluggishly with CO form on the catalyst surface under the oxidation conditions [19].

The Ru/MgO catalyst also undergoes rapid deactivation during CO oxidation in the absence of H₂ [20]. At 100°C, the CO conversion on a prereduced Ru/MgO sample decreased from 85 to <10% within 15–20 min. In the authors' opinion, the deactivation of this catalyst is due to ruthenium oxidation yielding an oxide phase.

In the above experiments on CO oxidation in excess hydrogen in the presence of H₂O and CO₂ in the catalyst surface ignition regime at comparatively high temperatures, we did not directly observe any decline of catalytic activity. However, as was indicated by indirect data, it did take place, though at a low rate.

Figure 6 illustrates the evolution of the residual CO concentration and of the gas temperatures at the catalyst (0.1% Ru/Al₂O₃) bed entrance and exit (sample 2 in Fig. 5). After the replacement of hydrogen with the reaction mixture (57th minute) and the ignition of the catalyst surface, the residual CO concentration does not exceed 15 ppm and even shows a decreasing trend (10–11 ppm at the end of the run) in spite of the high flow rate, the presence of considerable amounts of H₂O and CO₂, and a comparatively low O₂/CO ratio. Methane was not detected chromatographically in this experiment.

At the same time, the run of the temperature curves, specifically, the slow decrease in time of the gas temperature near the catalyst bed entrance and the corresponding increase of the gas temperature at the bed exit (Fig. 6), indicates that the hot spot moves toward the catalyst bed exit. This means that the activity of the catalyst decreases slowly with time on stream (see above). It would be expected that the gas temperature will then

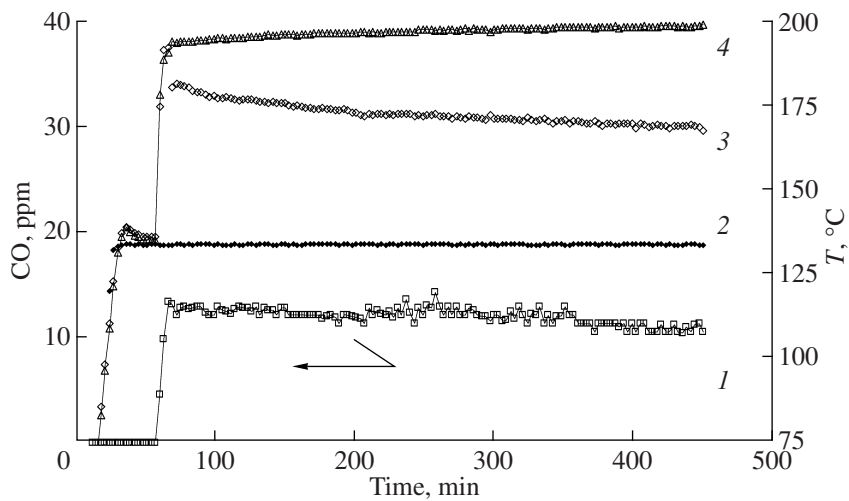


Fig. 6. Dynamics of the (1) residual CO concentration, (2) furnace temperature, (3) gas temperature at the bed exit, and (4) gas temperature at the bed entrance for selective CO oxidation on a 0.1% Ru/Al₂O₃ low-percentage catalyst (sample 2) in the surface ignition regime. Feed composition (vol %): CO, 0.77; O₂, 0.77; H₂, 57; CO₂, 18; H₂O, 21; N₂, balance. The gas flow rate is 90 l(g Cat)⁻¹ h⁻¹. H₂ is replaced with the feed in the 57th minute.

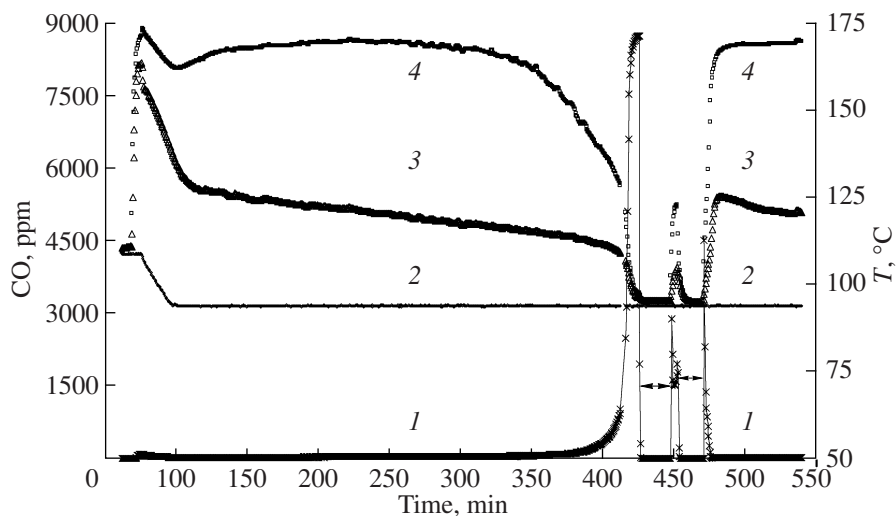


Fig. 7. Ignition, quenching, and activation of the 1% Ru/Al₂O₃ catalyst. In the 68th minute, humid H₂ is replaced with the feed mixture (for the mixture composition, see Fig. 1). From the 424th till the 446th minute and from the 452nd till the 469th minute, the catalyst is activated with humid hydrogen containing ~21 vol % water (see the arrows). (1) Residual CO concentration, (2) furnace temperature, (3) bed entrance temperature, and (4) bed exit temperature. The gas flow rate is 106 l(g Cat)⁻¹ h⁻¹.

decrease at the bed exit and this will finally cause the quenching of the surface and, accordingly, a dramatic decrease in the gas temperature and conversion.

The results of an experiment illustrating the displacement of the hot spot in the 1% Ru/Al₂O₃ bed and the quenching of the surface are presented in Fig. 7.

After the replacement of H₂ with the working mixture (68th minute), the surface ignited. Next, the furnace temperature was reduced from 109 to 94°C and was then maintained constant (as follows from Fig. 6, reducing the temperature is favorable for catalyst deactivation).

During the reaction conducted at this low furnace temperature, the gas temperature at the bed entrance gradually decreased. The gas temperature at the bed exit first increased slightly (in agreement with the shift of the hot spot) and then began to decrease. The runs of both curves reflect the slow deactivation of the catalyst. After ~400-min-long operation of the catalyst, the critical surface quenching temperature was reached and the reaction regime was changed: the gas temperature in the catalyst bed decreased down to the furnace temperature and the CO conversion fell dramatically. After being exposed to humid hydrogen for

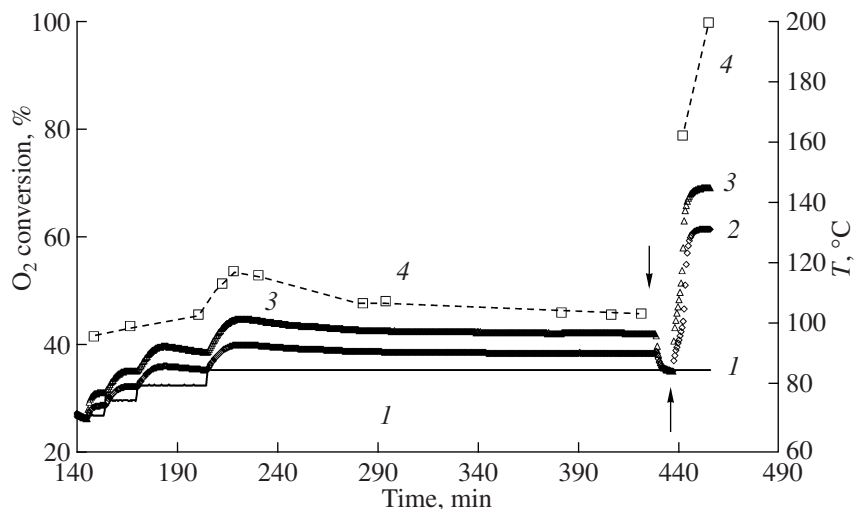


Fig. 8. H_2 oxidation on the 1% $\text{Ru}/\text{Al}_2\text{O}_3$ catalyst. The arrows point to the instants H_2 is replaced with the reaction mixture or vice versa. (1) Furnace temperature, (2) bed entrance temperature, (3) bed exit temperature, and (4) O_2 conversion. Feed composition (vol %): O_2 , 0.98; H_2 , 60; N_2 , balance. The gas flow rate is $54 \text{ l} (\text{g Cat})^{-1} \text{ h}^{-1}$.

20 min starting at the 424th minute, the catalyst partially regained its activity. After additional 17-min-long treatment starting at the 452nd minute, the catalyst surface ignited on replacing hydrogen with the reaction mixture and the initial catalytic activity was completely restored. Thus, hydrogen serves as a reactivating agent.

These results are not in conflict with the conclusion that the deactivation of the ruthenium catalyst is caused by some form of tightly bound oxygen appearing on the surface [19, 20]. Exposure to hydrogen brings the deactivated sites back into their active state. However, it is not impossible that the deactivation of the catalyst is due to the formation of tightly bound CO species on active sites and that these species are removed upon exposure to hydrogen or upon the admission of the feed. If this were the case, by eliminating CO from the reaction mixture, we could eliminate the cause of deactivation.

Figure 8 displays the results of the experiments in which hydrogen was oxidized in the absence of CO. The catalyst was heated in hydrogen to 130°C, cooled to 70°C, and purged with helium for 15 min. Next, the helium flow was replaced with the feed flow (145th minute; feed composition (vol %): O_2 , 0.98; H_2 , 60; N_2 as the balance gas) and the furnace temperature was raised in steps to 85°C. After the admission of the reaction mixture, the catalyst underwent heating so that the gas temperature at the bed exit was higher than the gas temperature at the bed entrance. As the furnace temperature was raised, the bed temperature grew and the oxygen conversion increased from 25.6% at a furnace temperature of 70°C (149th minute) to 40% at a furnace temperature of 85°C (231st minute; the furnace temperature was raised to 85°C in the 205th minute).

Holding the catalyst at the furnace temperature of 85°C for ~200 min caused a gradual decrease in the oxygen conversion to 31% and, accordingly, a decrease in the catalyst bed temperature. For example, the gas temperature at the bed exit is 101.2°C in the 231st minute and 96.9°C in the 426th minute. In the ~430th minute, the reaction mixture was replaced with hydrogen and the catalyst was held in flowing H_2 for ~8 min. Next, hydrogen was again replaced with the reaction mixture. This replacement of the hydrogen flow with the reaction mixture flow at a fixed furnace temperature caused the catalyst surface to ignite. The ignition event manifested itself as a dramatic increase of the O_2 conversion (to 99.7%) and of the gas temperature in the catalyst bed (Fig. 8).

Thus, short-term exposure to hydrogen activates the catalyst. Since there was no CO in the system in this experiment, the deactivation of the catalyst in the oxidation of CO and/or hydrogen can be due to some oxygen species tightly bound to the active sites.

For better illustration of the macrokinetic features of the system, we present, in Fig. 9, the complete record of experimental data whose fragment is shown in Fig. 1. In this experiment, the reactor was heated to 109°C under flowing hydrogen, the admission of water was switched on, and the H_2 flow was replaced with a feed ($\text{CO} + \text{O}_2 + \text{H}_2 + \text{N}_2$) flow (47th minute). After the admission of the feed, we observed the ignition of the catalyst surface, which manifested itself as a rapid heating of the reaction mixture (the exit and entrance temperatures were 200 and 131°C, respectively) and an equally rapid decrease of the residual CO concentration (down to ~130 ppm). Therefore, $T_{\text{cr}} < 109^\circ\text{C}$. The ignition regime persists as the furnace temperature is reduced to 99°C. Further reduction of the temperature

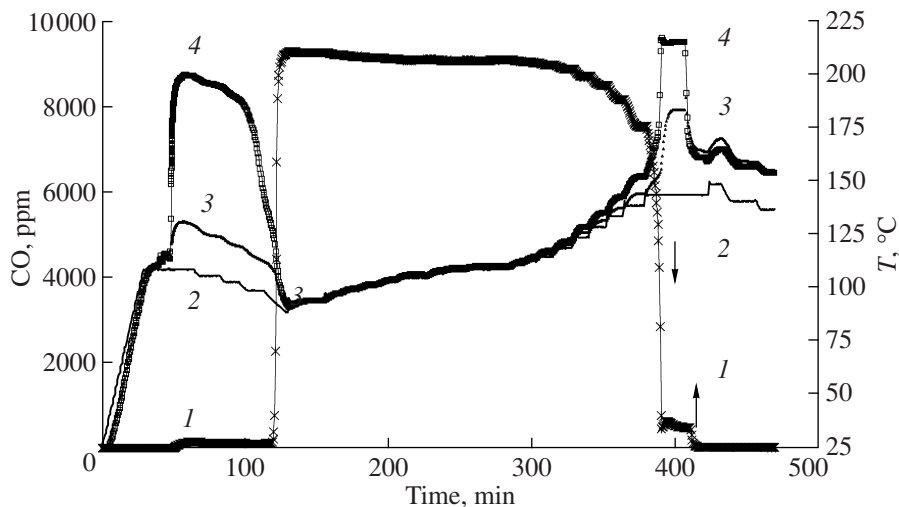


Fig. 9. Selective CO oxidation on the 1% Ru/Al₂O₃ catalyst: complete record of the experimental data presented in part in Fig. 1. In the 48th minute, H₂ is replaced with the reaction mixture. Between the 48th and the 407th minutes, the gas flow rate is 87 l (g Cat)⁻¹ h⁻¹; later, 17.5 l (g Cat)⁻¹ h⁻¹. (1) Residual CO concentration, (2) furnace temperature, (3) bed entrance temperature, and (4) bed exit temperature.

to 89°C caused the quenching of the surface (119th minute).

Subsequent heating of the furnace to 109°C did not cause the ignition of the catalyst surface (Fig. 9). Ignition was observed only at a furnace temperature of 144°C (380th minute). Since all oxidation conditions were identical, this dramatic change in the critical ignition temperature can be due solely to a change in the activity of the catalyst. Thus, the activity of the ruthenium catalyst depends strongly on the pretreatment procedure.

Decreasing the gas flow rate from 87 to 17.5 l (g Cat)⁻¹ h⁻¹ (407th minute) reduces the residual CO concentration in the catalyst surface ignition regime to ~20 ppm. A further decrease in the CO concentration can be achieved by reducing the furnace temperature without going beyond the ignition limits. This procedure (steps at 149, 141, and 137°C) allowed the residual CO concentration to be reduced to 12 ppm.

Thus, by establishing the catalyst surface ignition regime in some way, and by varying the gas flow rate and the furnace temperature within the ignition limits, it is possible to improve the performance of the selective CO oxidation process. The combination of the advantages of the low-percentage ruthenium catalyst and the selectivity gain provided by the catalyst surface ignition regime enabled us to remove CO almost completely (down to a level of 10–15 ppm; see Fig. 6) at gas flow rates of about 100 l (g Cat)⁻¹ h⁻¹ in the presence of H₂O and CO₂ (~20 vol % each).

ACKNOWLEDGMENTS

This work was supported by the Russian Foundation for Basic Research (grant no. 06-03-32848).

REFERENCES

1. Edwards, N., Ellis, S.R., Frost, J.C., Golunski, S.E., van Keulen, A.N.J., Lindewald, N.G., and Reinkingh, J.G., *J. Power Sources*, 1998, vol. 71, p. 123.
2. US Patent 6576208, 2003.
3. Echigo, M. and Tabata, T., *Appl. Catal., A*, 2003, vol. 251, p. 157.
4. Snytnikov, P.V., *Extended Abstract of Cand. Sci. (Chem.) Dissertation*, Novosibirsk: Inst. of Catalysis, 2004.
5. Eur. Patent 1485202, 2003.
6. Snytnikov, P.V., Sobyanin, V.A., Belyaev, V.D., Tsyrulnikov, P.G., Shitova, N.B., and Shlyapin, D.A., *Appl. Catal., A*, 2003, vol. 239, p. 149.
7. Kawatsu, S., *J. Power Sources*, 1998, vol. 71, p. 150.
8. Dudfield, C.D., Chen, R., and Adcock, P.L., *J. Power Sources*, 2000, vol. 86, p. 214.
9. Kipnis, M.A., Volnina, E.A., Samokhin, P.V., Lin, G.I., and Rozovskii, A.Ya., *Tezisy dokl. I Vseross. konf. "Khimiya dlya avtomobil'nogo transporta"* (Proc. 1st Russian Conf. on Chemistry for Automotive Applications), Novosibirsk, 2004, pp. 199.
10. Dudfield, C.D., Chen, R., and Adcock, P.L., *J. Power Sources*, 2000, vol. 85, p. 237.
11. Rosso, I., Galletti, C., Saracco, G., Garrone, E., and Specchia, V., *Appl. Catal., B*, 2004, vol. 48, p. 195.

12. Worner, A., Friedrich, C., and Tamme, R., *Appl. Catal.*, A, 2003, vol. 245, p. 1.
13. Han, Y.-F., Kahlich, M.J., Kinne, M., and Behm, R.J., *Phys. Chem. Chem. Phys.*, 2002, vol. 4, p. 389.
14. Rozovskii, A.Ya., Kipnis, M.A., Volnina, E.A., Lin, G.I., and Samokhin, P.V., *Kinet. Katal.*, 2004, vol. 45, no. 4, p. 654 [*Kinet. Catal.* (Engl. Transl.), vol. 45, no. 4, p. 618].
15. Rozovskii, A.Ya., Kipnis, M.A., Volnina, E.A., Lin, G.I., and Samokhin, P.V., *Kinet. Katal.* (in press).
16. Frank-Kamenetskii, D.A., *Diffuziya i teploperedacha v khimicheskoi kinetike* (Diffusion and Heat Transfer in Chemical Kinetics), Moscow: Nauka, 1967.
17. Rozovskii, A.Ya., *Kinetika topokhimicheskikh reaktsii* (Kinetics of Topochemical Reactions), Moscow: Nauka, 1980.
18. Zhilyaeva, N.A., Volnina, E.A., Shuikina, L.P., and Frolov, V.M., *Neftekhimiya*, 2000, vol. 40, no. 6, p. 422 [*Pet. Chem.* (Engl. Transl.), vol. 40, no. 6, p. 383].
19. Kiss, J.T. and Gonzalez, R.D., *J. Phys. Chem.*, 1984, vol. 88, p. 892.
20. Amann, J., Crihan, D., Knapp, M., Lundgren, E., Loffler, E., Muhler, M., Narknede, V., Over, H., Schmid, M., Seitsonen, A.P., and Varga, P., *Angew. Chem., Int. Ed. Engl.*, 2005, vol. 44, p. 917.